Inorg. Chem. **2009**, *48*, 1920−1927

Stability of [2]Pseudorotaxanes Templated Through Second-Sphere Coordination

Barry A. Blight, James A. Wisner,* and Michael C. Jennings

Department of Chemistry, The University of Western Ontario, 1151 Richmond Street, Chemistry Building, London, Ontario N6A 5B7, Canada

Received September 8, 2008

A series of nine *trans*-dichlorobis(pyridine)palladium(II) complexes were prepared (**2a-i**), containing different 4-substituted pyridine co-ligands. The association constants between these Pd-complexes and **1** were measured, and their values plotted against corresponding $\sigma_p°$ values. Measurement of the hydrogen bond acceptor capability of the chloride co-ligands revealed the presence of a linear free energy relationship between the electronic induction of a given 4-substituted pyridine co-ligand and the subsequent complexation strength in [2]pseudorotaxane formation. These trends also extended to *trans*-dibromobis(pyridine)palladium(II) (**3a-e**) and *trans*- dichlorobis(pyridine)platinum(II) complexes (**5a-e**) when plotted against $\sigma_p°$ values. In addition, solid-state structures of three [2]pseudorotaxanes (**1**·**2h**, **1**·**2i**, and **1**·**5e**) were determined by single crystal X-ray diffraction further confirming the viability of this template in forming interpenetrated molecular architectures.

Introduction

The successful synthesis of mechanically interlocked molecular species has rested on effective template strategies as a key element in their self-assembly.[1] [2]Pseudorotaxane complexes have played an important role as a testing ground in this regard.[2] [2]Pseudorotaxanes are composed of an equilibrating mixture of a "wheel-shaped" molecule interpenetrated by an "axle-shaped" molecule and are conceptual precursors to interlocked molecules with potential shuttling[3] or switching properties.[3a,4] A number of template strategies exist for [2]pseudorotaxane self-assembly that employ the use of complementary non-covalent interactions (hydrogen bonding,[1e,5] π-stacking,[1i,6] and hydrophobic interactions[7]) to populate the equilibrium in favor of [2]pseudorotaxane formation versus free components. These structures may then be rendered interlocked through "stoppering" of the termini of the axle component (forming a [2]otaxane) with sterically demanding groups,[1a,d,k,o,2c,8] or by connecting ("clipping") the termini (forming a [2]atenane)[1b,c,g,i,9] with the magnitude of the template interaction having a significant influence on the yields.

A number of accounts have described the self-assembly of [2]pseudorotaxanes using metal cations as a key participant in the arrangement/ordering process of the free components. In these cases, the metal cation was either incorporated into the backbone of the macrocyclic component (metal−ligand coordination),[10] arranged two components into an orthogonal

* To whom correspondence should be addressed. E-mail: jwisner@uwo.ca.

(1) (a) Ogino, H. *J. Am. Chem. Soc.* **1981**, *103*, 1303. (b) Hunter, C. A. *J. Am. Chem. Soc.* **1992**, *114*, 5303. (c) Collin, J.-P.; Dietrich-Buchecker, C.; Gaviña, P.; Jimenez-Molero, M. C.; Sauvage, J.-P. *Acc. Chem. Res.* **2001**, *34*, 477. (d) Wylie, R. S.; Macartney, D. H. *J. Am. Chem. Soc.* **1992**, *114*, 3136. (e) Ashton, P. R.; Campbell, P. J.; Chrystal, E. J. T.; Glink, P. T.; Menzer, S.; Philp, D.; Spencer, N.; Stoddart, J. F.; Tasker, P. A.; Williams, D. J. *Angew. Chem., Int. Ed. Engl.* **1995**, *34*, 1865. (f) Leigh, D. A.; Murphy, A.; Smart, J. P.; Slawin, A. M. Z. *Angew. Chem., Int. Ed. Engl.* **1997**, *36*, 728. (g) Johnston, A. G.; Leigh, D. A.; Pritchard, R. J.; Deegan, M. D. *Angew. Chem., Int. Ed. Engl.* **1995**, *34*, 1209. (h) Wisner, J. A.; Beer, P. D.; Drew, M. G. B.; Sambrook, M. R. *J. Am. Chem. Soc.* **2002**, *124*, 12469. (i) Kaiser, G.; Jarrosson, T.; Otto, S.; Ng, Y.-F.; Bond, A. D.; Sanders, J. K. M. *Angew. Chem., Int. Ed.* **2004**, *43*, 1959. (j) Jager, R.; Vögtle, F. *Angew. Chem., Int. Ed. Engl.* **1997**, *36*, 930. (k) Vögtle, F.; Duennwald, T.; Schmidt, T. *Acc. Chem. Res.* **1996**, *29*, 451. (l) Vögtle, F.; Meier, S.; Hoss, R. *Angew. Chem., Int. Ed. Engl.* **1992**, *31*, 1619. (m) Nepogodiev, S. A.; Stoddart, J. F. *Chem. Rev.* **1998**, *98*, 1959. (n) Jeppesen, J. O.; Perkins, J.; Becher, J.; Stoddart, J. F. *Org. Lett.* **2000**, *2*, 3547. (o) Anelli, P. L.; Ashton, P. R.; Ballardini, R.; Balzani, V.; Delgado, M.; Gandolfi, M. T.; Goodnow, T. T.; Kaifer, A. E.; Philp, D.; Pietraszkiewicz, M.; Prodi, L.; Reddington, M. V.; Slawin, A. M. Z.; Spencer, N.; Stoddart, J. F.; Vicent, C.; Williams, D. J. *J. Am. Chem. Soc.* **1992**, *114*, 193.

(2) For reviews see: (a) Glink, P. T.; Schiavo, C.; Stoddart, J. F.; Williams, D. J. *Chem. Commun.* **1996**, *13*, 1483. (b) Fyfe, M. C. T.; Stoddart, J. F. *Coord. Chem. Rev.* **1999**, *183*, 139. (c) Kim, K. *Chem. Soc. Rev.* **2002**, *31*, 96. (d) Osakada, K.; Sakano, T.; Horie, M.; Suzaki, Y. *Coord. Chem. Rev.* **2006**, *250*, 1012. (e) Beer, P. D.; Sambrook, M. R.; Curiel, D. *Chem. Commun.* **2006**, *20*, 2105. (f) Vikers, M. S.; Beer, P. D. *Chem. Soc. Rev.* **2007**, *36*, 211. (g) Loeb, S. J. *Chem. Soc. Rev.* **2007**, *36*, 226.

10.1021/ic801725u CCC: $40.75
Published on Web 02/03/2009

Scheme 1. Structural Representation of All [2]Pseudorotaxanes Investigated in This Study

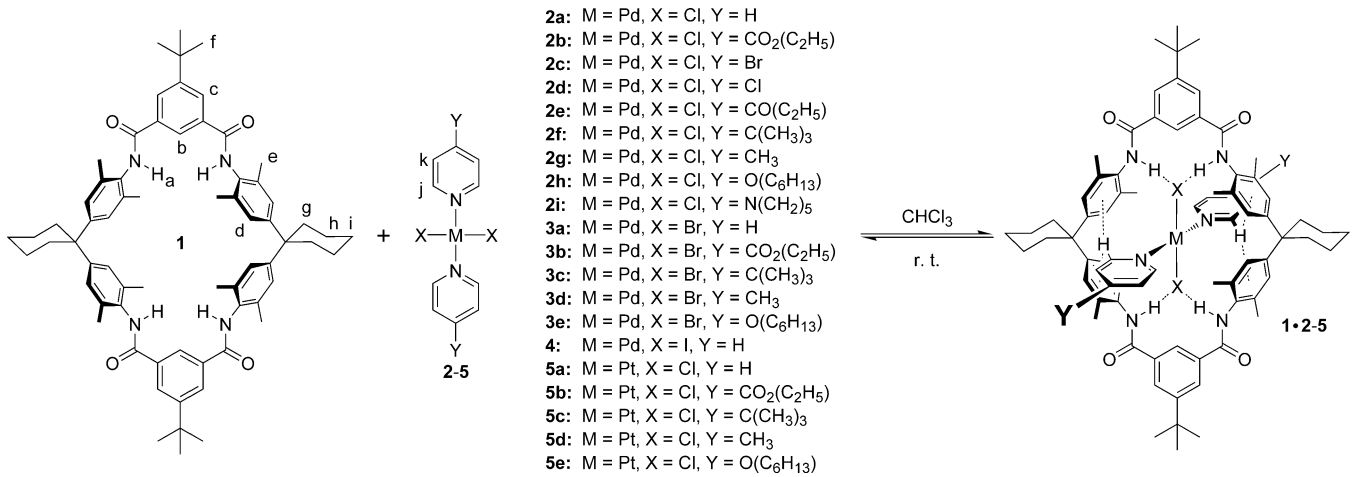

2a: M = Pd, X = Cl, Y = H
2b: M = Pd, X = Cl, Y = $CO_2(C_2H_5)$
2c: M = Pd, X = Cl, Y = Br
2d: M = Pd, X = Cl, Y = Cl
2e: M = Pd, X = Cl, Y = $CO(C_2H_5)$
2f: M = Pd, X = Cl, Y = $C(CH_3)_3$
2g: M = Pd, X = Cl, Y = CH_3
2h: M = Pd, X = Cl, Y = $O(C_6H_{13})$
2i: M = Pd, X = Cl, Y = $N(CH_2)_5$
3a: M = Pd, X = Br, Y = H
3b: M = Pd, X = Br, Y = $CO_2(C_2H_5)$
3c: M = Pd, X = Br, Y = $C(CH_3)_3$
3d: M = Pd, X = Br, Y = CH_3
3e: M = Pd, X = Br, Y = $O(C_6H_{13})$
4: M = Pd, X = I, Y = H
5a: M = Pt, X = Cl, Y = H
5b: M = Pt, X = Cl, Y = $CO_2(C_2H_5)$
5c: M = Pt, X = Cl, Y = $C(CH_3)_3$
5d: M = Pt, X = Cl, Y = CH_3
5e: M = Pt, X = Cl, Y = $O(C_6H_{13})$

and interpenetrated geometry (metal−ligand coordination),[11] or used to enhance the stability of a preformed metal-free [2]pseudorotaxane (secondary cation-dipole interactions).[6g,h] A common theme in these examples is the ligation of organic ligands to vacant coordination sites on the metal center, known as first-sphere or direct coordination. We have previously presented a preliminary investigation on the recognition of neutral *trans*-$PdCl_2L_2$ complexes by a well-known macrocyclic tetralactam **1** (Scheme 1).[12] Our investigation focused on hydrogen bonding between the halide ligands and the amide N−H groups of **1**, utilizing the metal complex's "second" sphere of coordination as the driving force for [2]pseudorotaxane formation. This strategy has since been employed simultaneously with simple nitrogen-based ligand exchange procedures to produce interlocked superstructures derived from the parent [2]pseudorotaxanes. The advantage here is that the hydrogen-bonded template remains separate from the nitrogen−palladium(II) coordinate bonds utilized as the interlocking connection points. For example, exchange of the pyridine co-ligands for 4-(3,5-di-*t*-butylbenzyl)oxypyridine or a bis-pyridyl bidentate ligand has resulted in the formation of [2]rotaxanes,[13,14] [2]catenanes,[14,15] and a molecular shuttle.[16] In this account, we revisit the formation of [2]pseudorotaxanes by this method to further investigate the effect substitution of the pyridine co-ligands has on complexation with **1**.

As mentioned, our previous study described [2]pseudorotaxane formation by combining various *trans*-dihalobis(pyridine)palladium(II) complexes with **1** in solution and examined the strength of complexation in relation to both the identity of the halide and the electron-donating nature of the pyridine co-ligands. A trend between the donating ability of the pyridine co-ligands into the metal center of the $PdCl_2Py_2$-axle component and the strength of complexation of axle with **1** was revealed (**1·2b**, 2400 (±140) M^{-1}; **1·2a**, 5000 (±200) M^{-1}; **1·2h**, 5500 (±45) M^{-1} in $CDCl_3$) when pyridine, ethyl-isonicotinate, and 4-hexyloxypyridine were employed as the co-ligands in the axle component (**2a**, **2b**, and **2h**, respectively). Since the observed trend in complexation strength of **1** with **2a**, **2b**, and **2h** was based on only these three axles, we have expanded this library to nine axles (**2a-i**) and can now confirm that a linear free-energy relationship exists between the strengths of association of **1·2a**−**1·2i** and the Hammett substituent constant σ_p°.[17] One can observe, through an intervening palladium(II) center, the inductive effects of a given para-substituted pyridine ligand (Scheme 1) on a *cis*-disposed chloride co-ligand by examining the extent of hydrogen bonding to the host macrocycle. We have also expanded the study to also include five palladium(II) dibromide complexes (**3a-e**) and five platinum(II) dichloride complexes (**5a-e**) anticipating a

(3) (a) Kay, E. R.; Leigh, D. A.; Zerbetto, F. *Angew. Chem., Int. Ed.* **2007**, *46*, 72, and references therein. (b) Mateo-Alonso, A.; Ehli, C.; Aminur Rahman, G. M.; Guldi, D. M.; Fioravanti, G.; Marcaccio, M.; Paolucci, F.; Prato, M. *Angew. Chem., Int. Ed.* **2007**, *46*, 3521. (c) Durola, F.; Sauvage, J.-P. *Angew. Chem., Int. Ed.* **2007**, *46*, 3537. (d) Abraham, W.; Buck, K.; Orda-Zgadzaj, M.; Schmidt-Schaeffer, S.; Grummet, U.-W. *Chem. Commun.* **2007**, 3094. (e) Aucagne, V.; Berna, J.; Crowley, J. D.; Goldup, S. M.; Haenni, K. D.; Leigh, D. A.; Lusby, P. J.; Ronaldson, V. E.; Slawin, A. M. Z.; Viterisi, A.; Walker, D. B. *J. Am. Chem. Soc.* **2007**, *129*, 11950. (f) Saha, S.; Flood, A. H.; Stoddart, J. F.; Impellizzeri, S.; Silvi, S.; Venturi, M.; Credi, A. *J. Am. Chem. Soc.* **2007**, *129*, 12159. (g) Crowley, J. D.; Leigh, D. A.; Lusby, P. J.; McBurney, R. T.; Perret-Aebi, L.-E.; Petzold, C.; Slawin, A. M. Z.; Symes, M. D. *J. Am. Chem. Soc.* **2007**, *129*, 15085. (h) Vella, S. J.; Tiburcio, J.; Loeb, S. J. *Chem. Commun.* **2007**, 4752. (i) Zhou, W.; Li, J.; He, X.; Li, C.; Lv, J.; Li, Y.; Wang, S.; Liu, H.; Zhu, D. *Chem.—Eur. J.* **2008**, *14*, 754. (j) Fioravanti, G.; Haraszkiewicz, N.; Kay, E. R.; Mendoza, S. M.; Bruno, C.; Marcaccio, M.; Wiering, P. G.; Paolucci, F.; Rudolf, P.; Bouwer, A. M.; Leigh, D. A. *J. Am. Chem. Soc.* **2008**, *130*, 2593.

(4) (a) Goddard, W. A., III; Kim, Y.-H. *J. Phys. Chem. C.* **2007**, *111*, 4831. (b) Tuncel, D.; Oezsar, O.; Tiftik, H. B.; Salih, B. *Chem. Commun.* **2007**, 1369. (c) Huang, Y.-L.; Hung, W.-C.; Lai, C.-C.; Liu, Y.-H.; Peng, S.-M.; Chiu, S.-H. *Angew. Chem., Int. Ed.* **2007**, *46*, 6629.

(5) (a) Kolchinski, A. G.; Busch, D. H.; Alcock, N. W. *J. Chem. Soc. Chem. Commun.* **1995**, 1289. (b) Clifford, T.; Abushamleh, A.; Busch, D. H. *Proc. Natl. Acad. Sci. U.S.A.* **2002**, *99*, 4830. (c) Ashton, P. R.; Chrystal, E. J. T.; Glink, P. T.; Menzer, S.; Shiavo, C.; Stoddart, J. F.; Tasker, P. A.; Williams, D. J. *Angew. Chem., Int. Ed. Engl.* **1995**, *34*, 1869. (d) Ashton, P. R.; Chrystal, E. J. T.; Glink, P. T.; Menzer, S.; Shiavo, C.; Spencer, N.; Stoddart, J. F.; Tasker, P. A.; White, A. J. P.; Williams, D. J. *Chem.—Eur. J.* **1996**, *2*, 709. (e) Ashton, P. R.; Fyfe, M. C. T.; Hickingbottom, S. K.; Stoddart, J. F.; White, A. J. P.; Williams, D. J. *J. Chem. Soc., Perkin Trans. 2.* **1998**, 2117. (f) Chiu, S.-H.; Liao, K.-S.; Su, J.-K. *Tetrahedron Lett.* **2004**, *45*, 213. (g) Wisner, J. A.; Beer, P. B.; Drew, M. G. B. *Angew. Chem., Int. Ed.* **2001**, *40*, 3606. (h) Wisner, J. A.; Beer, P. D.; Berry, N. G.; Tomapatanaget, B. *Proc. Natl. Acad. Sci. U.S.A.* **2002**, *99*, 4983. (i) Sambrook, M. R.; Beer, P. D.; Wisner, J. A.; Paul, R. L.; Cowley, A. R.; Szemes, F.; Drew, M. G. B. *J. Am. Chem. Soc.* **2005**, *127*, 2292. (j) Chang, S.-Y.; Kim, H. S.; Chang, K.-J.; Jeong, K.-S. *Org. Lett.* **2004**, *6*, 181.

reduced affinity between **1** and both series of axles. Moreover, X-ray quality single crystals were successfully grown of **1·2h**, **1·2i**, and **1·5c**, and their solid state structures are discussed.

Experimental Section

General Information. All reactions were performed in dry solvents, and under an inert $N_{2(g)}$ atmosphere. All organic reagents were purchased from Aldrich Chemical Co. including palladium(II) dibromide, while palladium(II) dichloride and potassium tetrachloroplatinate were purchased from Pressure Chemical Company and all used without further purification. NMR spectral analyses for characterization purposes were performed on a Varian Mercury 400 MHz instrument. ^{195}Pt NMR analyses were performed on a Varian Inova 400 MHz instrument. 1-D rotating-frame Overhauser enhancement spectroscopy (ROESY) experiments were performed on a Varian Inova 600 MHz instrument. ^{1}H NMR titration experiments were also performed on the Varian Inova 600 MHz instrument and performed with a constant concentration of the host **1** at 5×10^{-4} M and the addition of appropriate aliquots of a solution of guests **2**−**5** at 5×10^{-3} M (with background host concentration) using Hamilton Gastight microlitre syringes. All titrations were performed three times, and the average values of the association constants obtained are reported. Titration data from the observation of the appropriate protons H_a-H_f were analyzed with the program EQNMR[21] and fit a 2:1 binding model with excellent agreement (Rf = 0.05%). Electrospray ionization mass determinations with samples dissolved in a chloroform/methanol matrix were performed with Micromass LCT instrumentation. Please refer to the Cambridge Crystallographic Database or the electronic Supporting Information for the electronic CIF files: CCDC-691009 (**1·2h**), CCDC-681010 (**1·2i**), and CCDC-681011 (**1·5e**). The syntheses of **1**,[22] **2a**,[23] **2b**,[24] **2c**,[25] **2d**,[25] **2f**,[26] **2g**,[27] **2h**,[28] **3a**,[29] **3d**,[29] **4**,[30] **5a**,[31] **5c**,[31] and **5d**[31] have been previously reported, while **2e**, **2i**, **3b**, **3c**, **3e**, **5b**, and **5e** were newly synthesized with procedures described herein. The purity of the newly synthesized complexes was confirmed by thin-layer chromatography (TLC) analysis in two different solvent systems (single spot in both), ^{1}H NMR (single set of peaks), and HR-ESI-MS analysis. Additionally, **2b** and **2h** were synthesized in the manner reported here because of the straightforwardness of this procedure.

X-ray Crystallography. Single crystal X-ray diffraction data, for **1·2h**,**·1 2i**, and **1·5e** were obtained from a programmed hemisphere scan routine on a Nonius Kappa-CCD diffractometer (Table 1). The unit cell parameters were calculated and refined from the full data set. Crystal cell refinement and data reduction were carried out using DENZO (Nonius B.V., 1998). The data were scaled using SCALEPACK (Nonius B.V., 1998). The solutions for **1·2h**, **1·2i**, and **1·5e** were all solved by direct methods, followed by difference Fourier syntheses to find the remaining atoms in each subsequent structure. Refinement was with full-matrix least-squares methods using SHELXTL-NT 6.1 (Sheldrick, G. M., Madison, WI, **2000**). The organic material and the metal center(s) were very well resolved in both structures. All of the non-hydrogen atoms were refined with anisotropic thermal parameters. The hydrogen atom positions were calculated geometrically and were included as riding on their respective carbon atoms. Alert level A's associated with **1·2i** are regarding larger than normal anisotropic displacement parameters of one *t*-butyl group of a macrocyclic component and some solvent molecules. In addition, because of the labeling

(6) (a) Aneli, P. L.; Ashton, P. R.; Spencer, N.; Slawin, A. M. Z.; Stoddart, J. F.; Williams, D. J. *Angew. Chem., Int. Ed. Engl.* **1991**, *30*, 1036. (b) Reddington, M. V.; Slawin, A. M. Z.; Spencer, N.; Stoddart, J. F.; Vicent, C.; Williams, D. J. *J. Chem. Soc., Chem. Commun.* **1991**, 630. (c) Ashton, P. R.; Philp, D.; Spencer, N.; Stoddart, J. F. *J. Chem. Soc., Chem. Commun.* **1991**, 1677. (d) Ashton, P. R.; Philp, D.; Reddington, M. V.; Slawin, A. M. Z.; Spencer, N.; Stoddart, J. F.; Williams, D. J. *J. Chem. Soc., Chem. Commun.* **1991**, 1680. (e) Loeb, S. J.; Wisner, J. A. *Angew. Chem., Int. Ed.* **1998**, *37*, 2838. (f) Loeb, S. J.; Tiburcio, J.; Vella, S. J.; Wisner, J. A. *Org. Biomol. Chem.* **2006**, *4*, 667. (g) Pascu, S.; Jarrosson, T.; Naumann, C.; Otto, S.; Kaiser, G.; Sanders, J. K. M. *New J. Chem.* **2005**, *29*, 80. (h) Pascu, S.; Naumann, C.; Kaiser, G.; Bond, A. D.; Sanders, J. K. M.; Jarrosson, T. *Dalton. Trans.* **2007**, 3874.

(7) (a) Yonemura, H.; Saito, H.; Matsushima, S.; Nakamura, H.; Matsuo, T. *Tetrahedron Lett.* **1989**, *30*, 3143. (b) Saito, H.; Yonemura, H.; Nakamura, H.; Matsuo, T. *Chem. Lett.* **1990**, 535. (c) Harada, A.; Li, J.; Kamachi, M. *Nature* **1992**, *356*, 325. (d) Mirzoian, A.; Kaifer, A. E. *Chem.*−*Eur. J.* **1997**, *3*, 1052. (e) Smith, A. C.; Macartney, D. H. *J. Org. Chem.* **1998**, *63*, 9243. (f) Lyon, A. P.; Banton, N. J.; Macartney, D. H. *Can. J. Chem.* **1998**, *76*, 843. (g) Jeon, Y.-M.; Whang, D.; Kim, J.; Kim, K. *Chem. Lett.* **1996**, 503.

(8) (a) Wylie, R. S.; Macartney, D. H. *Supramol. Chem.* **1993**, *3*, 29. (b) Macartney, D. H.; Waddling, C. A. *Inorg. Chem.* **1994**, *33*, 5912. (c) Hannak, R. B.; Färber, G.; Konrat, R.; Kräuter, B. *J. Am. Chem. Soc.* **1997**, *119*, 2313. (d) Brown, C. L.; Philp, D.; Stoddart, J. F. *Synlett* **1991**, 459–461. (e) Philp, D.; Stoddart, J. F. *Synlett* **1991**, 445. (f) Ashton, P. R.; Grognuz, M.; Slawin, A. M. Z.; Stoddart, J. F.; Williams, D. J. *Tetrahedron Lett.* **1991**, *32*, 6235. (g) Bermudez, V.; Capron, N.; Gase, T.; Gatti, F. G.; Kajzar, F.; Leigh, D. A.; Zerbetto, F.; Zhang, S. *Nature* **2000**, *406*, 608. (h) Gunter, M. J.; Bampos, N.; Johnstone, K. D.; Sanders, J. K. M. *New J. Chem.* **2001**, *25*, 166. (i) Loeb, S. J.; Wisner, J. A. *Chem. Commun.* **1998**, 2756. (j) Davidson, G. J. E.; Loeb, S. J.; Parekh, N. A.; Wisner, J. A. *J. Chem. Soc., Dalton Trans.* **2001**, 3135.

(9) (a) Leigh, D. A.; Wong, J. K. Y.; Dehez, F.; Zerbetto, F. *Nature* **2003**, *424*, 174. (b) Hernández, J. V.; Kay, E. R.; Leigh, D. A. *Science* **2004**, *306*, 1532. (c) Sambrook, M. R.; Beer, P. D.; Wisner, J. A.; Paul, R. L.; Cowley, A. R. *J. Am. Chem. Soc.* **2004**, *126*, 15364. (d) Ng, K.-Y.; Cowley, A. R.; Beer, P. D. *Chem. Commun.* **2006**, 3676. (e) Hubbard, A. L.; Davidson, G. J. E.; Patel, R. H.; Wisner, J. A.; Loeb, S. J. *Chem. Commun.* **2004**, 138.

(10) (a) Blanco, V.; Chas, M.; Abella, D.; Pía, E.; Platas-Iglesias, C.; Peinador, C.; Quintela, J. M. *Org. Lett.* **2008**, *10*, 409. (b) Blanco, V.; Chas, M.; Abella, D.; Pía, E.; Blanco, G.; Fernandez, A.; Platas-Iglesias, C.; Peinador, C.; Quintela, J. M. *Chem.*−*Eur. J.* **2007**, *13*, 8572.

(11) (a) Dietrich-Buchecker, C. O.; Sauvage, J.-P. *Tetrahedron Lett.* **1983**, *24*, 5095. (b) Sleiman, H.; Baxter, P. N. W.; Lehn, J.-M.; Airola, K.; Rissanen, K. *Inorg. Chem.* **1997**, *36*, 4734.

(12) Blight, B. A.; Van Noortwyk, K. A.; Wisner, J. A.; Jennings, M. C. *Angew. Chem., Int. Ed.* **2005**, *44*, 1499.

(13) Blight, B. A.; Wisner, J. A.; Jennings, M. C. *Chem. Commun.* **2006**, 4583.

(14) Blight, B. A.; Wisner, J. A.; Jennings, M. C. *Can. J. Chem.* **2009**, *87*, 205−211.

(15) Blight, B. A.; Wisner, J. A.; Jennings, M. C. *Angew. Chem., Int. Ed.* **2007**, *46*, 2835.

(16) Blight, B. A.; Xu, W.; Wisner, J. A.; Jennings, M. C. *Inorg. Chem.* **2007**, *46*, 8445.

(17) (a) Taft, R. W. *J. Phys. Chem.* **1960**, *64*, 1805. (b) Hansch, C.; Leo, A.; Taft, R. W. *Chem. Rev.* **1991**, *91*, 165.

(18) Exner, O. In *Correlation Analysis in Chemistry*; Chapman, N. B., Shorter, J., Eds.; Plenum: London, 1978; Chapter 10.

(19) The least squares plane of **1** is defined by the four carbonyl carbons.

(20) Measured by calculating the angle from the normal between the planes perpendicular to the lines defined by (i) the Cl-Pd-Cl axis and (ii) the line described by the two carbonyl-substituted carbon atoms of the isophthalamide ring.

(21) Hynes, M. J. *J. Chem. Soc., Dalton Trans.* **1993**, 311.

(22) Fischer, C.; Nieger, M.; Mogck, O.; Böhmer, V.; Ungaro, R.; Vögtle, F. *Eur. J. Org. Chem.* **1998**, 155.

(23) Rajput, J.; Moss, J. R.; Hutton, A. T.; Henfricks, D. T.; Arendse, C. E.; Imrie, C. *J. Organomet. Chem.* **2004**, *689*, 1553.

(24) Kong, P.; Rochon, F. D. *Can. J. Chem.* **1981**, *59*, 3293.

(25) Zordan, F.; Bramer, L. *Cryst. Growth Des.* **2006**, *6*, 1374.

(26) Le Stang, S.; Paul, F.; Lapinte, C. *Inorg. Chim. Acta* **1999**, *291*, 403.

(27) Adams, C. J.; Crawford, P. C.; Orpen, A. G.; Podesta, T. J.; Salt, B. *Chem. Commun.* **2005**, 2457.

(28) Wehman, P.; Dol, D. C.; Moon, E. R.; Kamer, P. C. J.; van Leeuwen, P. W. M. N.; Fraanje, J.; Goubitz, K. *Organometallics* **1994**, *13*, 4856.

Table 1. Crystal Data, Solution, and Refinement Parameters for **1·2h**,·**1 2i**, and **1·5e**

compound	**1·2h**	**1·2i**	**1·5e**
CCDC number	681009	681010	681011
empirical formula	$C_{90}H_{114}Cl_2N_6O_6Pd$	$C_{91.5}H_{111.5}Cl_{12.5}N_8O_4Pd$(**1·2i**·3.5$CHCl_3$·$H_2O$)	$C_{90}H_{114}Cl_2N_6O_6Pt$
formula weight	1553.17	1936.91	1641.86
crystal description	yellow prism	yellow plate	colorless plate
crystal size (mm)	0.28 × 0.28 × 0.15	0.40 × 0.13 × 0.05	0.28 × 0.23 × 0.03
crystal system	triclinic	triclinic	triclinic
space group	*P*2(1)/*n*	$P\bar{1}$	*P*2(1)/*n*
a (Å)	12.3713(6)	16.4463(2)	12.3833(4)
b (Å)	16.4045(7)	18.2388(2)	16.4284(3)
c (Å)	20.7926(9)	32.9736(4)	20.8099(5)
α (deg)	90	81.672(5)	90
β (deg)	106.068(3)	80.221(6)	106.077(2)
γ (deg)	90	87.215(6)	90
Z	2	4	2
cell volume (Å^3)	4054.9(3)	9641.4(2)	4067.59(18)
density calculated (g cm^{-3})	1.272	1.334	1.341
μ (mm^{-1})	0.352	0.591	1.848
independent reflections (R_{int})	7139 (0.061)	33952 (0.0680)	8312 (0.0760)
data/restraints/parameters	7139/0/475	33952/0/2135	8312/0/475
goodness-of-fit on F^2	1.046	1.083	1.070
final R_1 [$F^2 > 2\sigma F^2$]	0.0536	0.0737	0.0455
final wR_2 [$F^2 > 2\sigma F^2$]	0.1342	0.2063	0.11203
final R_1 (all data)	0.0851	0.1193	0.0751
final wR_2 (all data)	0.1522	0.22344	0.1332
residuals peak/hole (e/Å^3)	1.183/−0.635	3.734/−1.331	1.049/−1.456

restrictions of SHELXTL-NT 6.1 an unconventional method of atom numbering in **1·2i** was required. Macrocycle A and Pd(1) is associated axle containing the 100 series of atoms, while macrocycle B and Pd(2) is associated axle containing the 200 series of atoms. Data copies of CCDC-681009 (**1·2h**), CCDC-681010 (**1·2i**), and CCDC-681011 (**1·5e**) can be obtained free of charge on application to CCDC, 12 Union Road, Cambridge CB21EZ, U.K. (fax: (0.44) 1223−336−033; e-mail: deposit@ccdc.cam.ac.uk).

Procedures. General Procedure for the Preparation of 2b, 2e, 2h, 2i, 3b, 3c, and 3e. Trans-dihalobis(benzonitrile)palladium(II) ($PdCl_2(NCPh)_2$[32] or $PdBr_2(NCPh)_2$[32]) (0.16 mmol) was dissolved in acetonitrile (2 mL). The appropriate pyridine co-ligand (0.32 mmol) dissolved in acetonitrile (1 mL) was then added dropwise over 2 min and allowed to stir for 2 h. The resulting precipitate was filtered and washed with acetonitrile (10 mL).

***trans*-Dichlorobis(ethyl-iso-nicotinate)palladium(II) 2b.** 83% yield; ^{1}H NMR ($CDCl_3$, 400 MHz) δ 9.00 (d, J = 8 Hz, 4H), 7.90 (d, J = 8 Hz, 4H), 4.44 (qr, J = 8 Hz, 4H), 1.41 (t, J = 8 Hz, 6H). ^{13}C NMR ($CDCl_3$, 100 MHz) δ 163.2, 154.1, 139.9, 124.2, 62.6, 14.1. LR-ESI-MS [M + Na]$^+$ *m*/*z*: 503.1.

***trans*-Dichlorobis(4-proponylpyridine)palladium(II) 2e.** 88% yield; ^{1}H NMR ($CDCl_3$, 400 MHz) δ 9.03 (d, J = 8 Hz, 4H), 7.78 (d, J = 8 Hz, 4H), 3.00 (qr, J = 8 Hz, 4H), 1.24 (t, J = 8 Hz, 6H). ^{13}C NMR ($CDCl_3$, 100 MHz) δ 178.1, 162.3, 154.5, 122.4, 27.8, 8.8. HR-ESI-MS calcd for [M + Na]$^+$ $C_{16}H_{18}N_2Cl_2NaO_2Pd$ (found): 467.9694 (467.9686).

***trans*-Dichlorobis(4-*n*-hexyloxy-pyridine)palladium(II) 2h.** 72% yield; ^{1}H NMR ($CDCl_3$, 400 MHz) δ 8.55 (d, J = 8 Hz, 4H), 6.78 (d, J = 8 Hz, 4H), 4.01 (t, J = 8 Hz, 4H), 1.78 (qi, J = 8 Hz 4H) 1.42 (qi J = 8 Hz, 4H), 1.32 (m, 8H), 0.90 (t, J = 8 Hz, 6H). ^{13}C NMR ($CDCl_3$, 100 MHz) δ 166.6, 153.8, 111.4, 69.0, 31.3, 28.5, 25.4, 22.5, 14.0. LR-ESI-MS [M + H]$^+$ *m*/*z*: 501.1.

***trans*-Dichlorobis(4-*N*-pipyridylpyridine)palladium(II) 2i.** 91% yield; ^{1}H NMR ($CDCl_3$, 400 MHz) δ 8.21 (d, J = 8 Hz, 4H), 6.51 (d, J = 8 Hz, 4H), 3.36 (dd, J = 8 and 8 Hz, 8H), 1.66 (m, 4H), 1.60 (m, 8H). ^{13}C NMR ($CDCl_3$, 100 MHz) δ 154.5, 152.0, 108.1, 47.0, 25.0, 24.1. HR-ESI-MS calcd for [M + Na]$^+$ $C_{20}H_{28}N_4Cl_2NaPd$ (found): 521.0629 (521.0652).

***trans*-Dibromobis(ethyl-iso-nicotinate)palladium(II) 3b.** 71% yield; ^{1}H NMR ($CDCl_3$, 400 MHz) δ 9.05 (d, J = 8 Hz, 4H), 7.88 (d, J = 8 Hz, 4H), 4.43 (qr, J = 8 Hz, 4H), 1.40 (t, J = 8 Hz 6H). ^{13}C NMR ($CDCl_3$, 100 MHz) δ 163.2, 155.0, 139.8, 124.2, 62.6, 14.1. HR-ESI-MS calcd for [M + Na]$^+$ $C_{16}H_{18}N_2Br_2NaO_4Pd$ (found): 587.8582 (587.8561).

***trans*-Dibromobis(4-*t*-butylpyridine)palladium(II) 3c.** 86% yield; ^{1}H NMR ($CDCl_3$, 400 MHz) δ 8.73 (d, J = 8 Hz, 4H), 7.28 (d, J = 8 Hz, 4H), 1.29 (s, 9H). ^{13}C NMR ($CDCl_3$, 100 MHz) δ 153.6, 145.2, 122.3, 35.7, 31.2. HR-ESI-MS calcd for [M + Na]$^+$ $C_{18}H_{26}N_2Br_2NaPd$ (found): 554.9401 (554.9423).

***trans*-Dibromobis(4-*n*-hexyloxy-pyridine)palladium(II) 3e.** 65% yield; ^{1}H NMR ($CDCl_3$, 400 MHz) δ 8.60 (d, J = 8 Hz, 4H), 6.77 (d, J = 8 Hz, 4H), 4.00 (t, J = 8 Hz, 4H), 1.78 (qi, J = 8 Hz 4H), 1.42 (qi J = 8 Hz, 4H), 1.32 (m, 8H), 0.90 (t, J = 8 Hz, 6H). ^{13}C NMR ($CDCl_3$, 100 MHz) δ 166.5, 154.8, 111.6, 69.0, 31.3, 28.5, 25.4, 22.5, 14.0. HR-ESI-MS [M + Na]$^+$ $C_{22}H_{34}N_2Br_2NaO_2Pd$ (found): 642.9925 (642.9913).

General Procedure for the Preparation of 5b and 5c. Bis-dimethylsulfide platinum(II) dichloride (0.15 mmol) and the appropriate ligand (0.30 mmol) were dissolved in 1,2-dichloroethane and refluxed for 36 h. The reaction mixture was concentrated under reduced pressure and subject to column chromatography (dichloromethane as eluant). In both cases, the leading band (yellow) was determined to be the *trans*-isomer via ^{195}Pt NMR experiments.[31a]

***trans*-Dichlorobis(ethyl-iso-nicotinate)platinum(II) 5b.** 56% yield; ^{1}H NMR ($CDCl_3$, 400 MHz) δ 9.07 (d, J = 8 Hz, 4H), 7.87 (d, J = 8 Hz, 4H), 4.44 (qr, J = 8 Hz, 4H), 1.41 (t, J = 8 Hz 6H). ^{13}C NMR ($CDCl_3$, 100 MHz) δ 163.2, 154.4, 139.6, 124.5, 62.6, 14.1. ^{195}Pt NMR ($CDCl_3$, 86 MHz) δ −1941.9. HR-ESI-MS calcd for [M + Na]$^+$ $C_{16}H_{18}N_2Cl_2NaO_4Pt$ (found): 589.0168 (589.0148).

***trans*-Dichlorobis(4-*n*-hexyloxy-pyridine)platinum(II) 5e.** 48% yield; ^{1}H NMR ($CDCl_3$, 400 MHz) δ 8.63 (d, J = 8 Hz, 4H), 6.75 (d, J = 8 Hz, 4H), 4.02 (t, J = 8 Hz, 4H), 1.78 (qi, J = 8 Hz 4H), 1.43 (qi J = 8 Hz, 4H), 1.32 (m, 8H), 0.90 (t, J = 8 Hz, 6H). ^{13}C NMR ($CDCl_3$, 100 MHz) δ 166.3, 154.0, 111.6, 69.0, 31.3, 28.5,

(29) *Gmelins Handbuch der anorganischen Chemie*; Verlag Chemie: Berlin, 1942; Vol. LXV, pp 387.

Table 2. ^{1}H NMR Chemical Shift Values of H_a-H_d, H_j, and H_k in $CDCl_3$ at 298 K for Equimolar Concentrations of **1** with Axles **2** − **5**

	δ in ppm at equimolar comcentrations 5×10^{-4} M ($\triangle\delta$ 1:1)		
complex	H_a	H_d	H_e
1·2a	7.74 (0.62)	7.12 (0.15)	8.18 (−0.63)
1·2b	7.56 (0.44)	7.1 (0.13)	8.56 (−0.49)
1·2c	7.43 (0.31)	7.06 (0.09)	8.17 (−0.46)
1·2d	7.46 (0.34)	7.06 (0.09)	8.18 (−0.56)
1·2e	7.45 (0.33)	7.06 (0.09)	8.52 (−0.51)
1·2f	7.78 (0.66)	7.11 (0.14)	8.12 (−0.56)
1·2g	7.80 (0.68)	7.12 (0.15)	7.80 (−0.83)
1·2h	8.00 (0.88)	7.19 (0.22)	8.24 (−0.34)
1·2i	8.09 (0.97)	7.22 (0.25)	8.14 (−0.07)
1·3a	7.30 (0.18)	7.02 (0.05)	8.76 (−0.14)
1·3b	7.22 (0.10)	7.01 (0.04)	8.93 (−0.13)
1·3c	7.21 (0.09)	7.03 (0.06)	8.48 (−0.21
1·3d	7.28 (0.20)	7.03 (0.06)	8.42 (−0.32)
1·3e	7.51 (0.39)	7.03 (0.06)	8.55 (−0.05)
4	7.14 (0.02)	6.98 (0.01)	6.92 (−0.01)
1·5a	7.50 (0.38)	7.06 (0.09)	8.28 (−0.48)
1·5b	7.39 (0.27)	7.05 (0.08)	8.67 (−0.41)
1·5c	7.41 (0.29)	7.05 (0.08)	8.29 (−0.45)
1·5d	7.44 (0.32)	7.06 (0.09)	8.26 (−0.46)
1·5e	7.53 (0.41)	7.07 (0.10)	8.16 (−0.48)

25.4, 22.5, 14.0. ^{195}Pt NMR($CDCl_3$, 86 MHz) −1910.3. HR-ESI-MS calcd for $[M + Na]^+$ $C_{22}H_{34}N_2Cl_2NaO_2Pt$ (found): 645.1522 (645.1514).

Results and Discussion

Solution Phase ^{1}H NMR Binding Studies. Upon isolation of the metal complexes in question (**2a**-**i**, **3a**-**e**, **4**, and **5a**-**e**) ^{1}H NMR spectra of solutions ($CDCl_3$) containing equimolar concentrations of **1** and axle were obtained, which displayed a single set of signals that did not correspond to those of the free components. This indicated to us that this [2]pseudorotaxane formation process is fast on the NMR time scale in all cases, resulting in spectra with a single set of average weighted signals for complexed and uncomplexed components. This differs greatly from systems that undergo slow exchange, which display resonances of all three distinct species (free components and the host−guest complex) simultaneously. Table 2 details the chemical shifts of diagnostic protons H_a, H_d, and H_j observed for each supramolecular complex at equimolar concentrations of **1** and axle.

The largest overall chemical shift perturbation of **1** as a result of host−guest complexation is observed for H_a, which is significantly deshielded because of its participation in hydrogen bonding to the chloride ligands, and likely the primary non-covalent interaction responsible for the formation of these interpenetrated species. H_j of the axle component also shows considerable shielding caused by C−H···π interactions with diphenylcyclohexyl sidewalls of **1**, which further results in the deshielding of H_d. In addition to the evidence interpreted from the ^{1}H NMR data, a 1-D ROESY experiment (Figure 1) performed on complex **1·2a** displays through-space NOE signals upon saturation of H_j, corresponding to H_d and H_e of **1** further supporting the presence of these attractive C−H···π interactions, as well as a weak NOE with H_a consistent with the interpenetrated complex geometry in solution (note: the NOE produced for H_k is an artifact of scalar coupling between H_j and H_k).^{1}H NMR

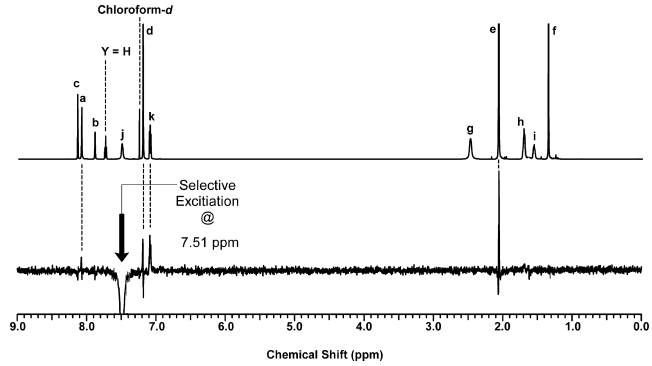

Figure 1. ^{1}H NMR (top) and 1-D ROESY (bottom) spectra ($CDCl_3$, 600 MHz, 298 K) of a 2.5×10^{-2} M solution of **1** and **2a**. Excitation at 7.51 ppm (H_j) produces notable NOE interactions with protons H_d, H_e, and H_k (see text).

Table 3. Association Constants ($K_{1:1}$ and $K_{2:1}$) and Gibbs Free Energies of Complexation for [2]Pseudorotaxanes **1·2a**-**i**, **1·3a**-**d**, **1·4**, and **1·5a**-**d** ($CDCl_3$, 298 K)[a]

complex	$K_{1:1}$ (M^{-1})	$-\Delta G_{1:1}$ (kJ mol^{-1})	$K_{2:1}$ (M^{-1})	$-\Delta G_{2:1}$ (kJ mol^{-1})
1·2a	5.0×10^3 (140)	21.1	2.0×10^2 (26)	13.1
1·2b	2.4×10^3 (200)	19.3	4.5×10^2 (22)	15.1
1·2c	2.9×10^3 (79)	19.8	6.9×10^2 (23)	16.2
1·2d	3.1×10^3 (31)	19.9	1.0×10^3 (102)	17.1
1·2e	3.3×10^3 (110)	20.1	5.8×10^2 (36)	15.8
1·2f	5.1×10^3 (41)	21.2	2.0×10^2 (18)	13.1
1·2g	5.4×10^3 (160)	21.3	1.8×10^2 (13)	12.9
1·2h	5.5×10^3 (45)	21.3	1.8×10^2 (9)	12.9
1·2i	6.8×10^3 (130)	21.9	7.3×10^1 (3)	10.6
1·3a	7.5×10^2 (13)	16.4	1.1×10^2 (2)	11.6
1·3b	1.8×10^2 (19)	12.9	5.5×10^1 (1)	9.9
1·3c	1.4×10^3 (71)	17.9	2.7×10^2 (3)	13.9
1·3d	1.2×10^3 (90)	17.6	2.8×10^2 (2)	14.0
1·3e	2.3×10^3 (80)	19.2	1.5×10^2 (4)	12.4
4	4.0×10^1 (3.2)	9.1		
1·5a	2.9×10^3 (65)	19.8	1.5×10^2 (5)	12.4
1·5b	1.9×10^3 (110)	18.7	1.0×10^2 (9)	11.4
1·5c	3.0×10^3 (54)	19.8	2.5×10^2 (14)	13.7
1·5d	3.6×10^3 (47)	20.3	1.8×10^2 (4)	12.9
1·5e	4.7×10^3 (49)	20.9	1.7×10^2 (8)	12.7

[a] Standard deviations from three trials are listed in brackets after the $K_{1:1}$ and $K_{2:1}$ values.

titration experiments were performed in $CDCl_3$ to determine the binding strengths (K_a) of each host−guest pair. In all cases, except **1·4**, both a 1:1 and a weaker 2:1 equilibria (macrocycle:axle) exist. The structure of this minor 2:1 equilibrium is likely a partially interpenetrated arrangement incorporating two macrocycles (one for each halide of the axle component), which is supported by the solid-state structure of a macrocyclic metal complex previously reported.[15] Table 3 details the association constants ($K_{1:1}$ and $K_{2:1}$) and Gibbs free energy of complexation measured for each of the 20 host−guest complexes.

Examination of the binding strengths reveals the intuitive dependence of K_a on the *para*-substituent character of the pyridine co-ligands. Association constants for 1:1 complexation of **1** with axles **2a**-**2i** range from 2400 (±200) M^{-1} (**1·2b**) to 6800 (±130) M^{-1} (**1·2i**) and when plotted with the Hammett substituent constant σ_p° yields a good linear correlation ($r^2 = 0.93$). We have chosen to use values of σ_p°, taken from Exner[18] rather than σ as they have been defined to express the isolated inductive effects of individual substituents in the absence of any resonance contributions

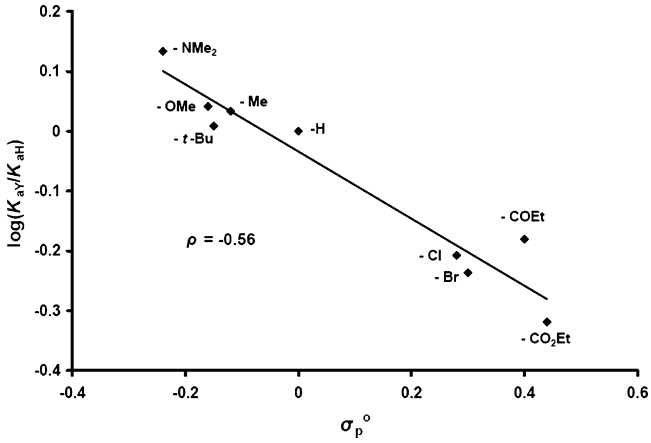

Figure 2. Hammett correlation between $\log(K_{aY}/K_{aH})$ and σ_p° at 298 K in $CDCl_3$ for [2]pseudorotaxanes composed of **1** and **2a**-**i** ($r^2 = 0.93$).

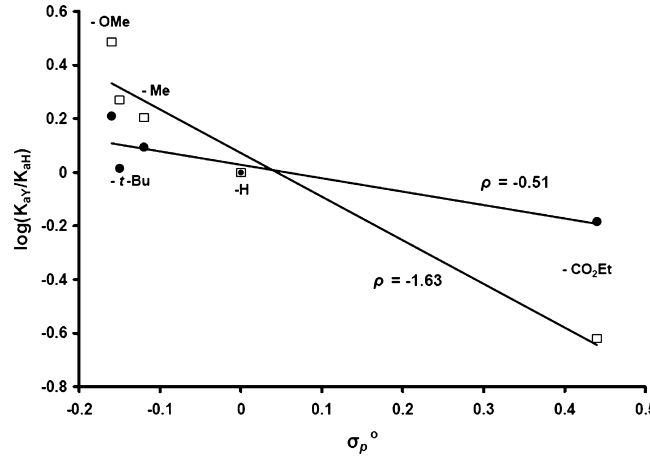

Figure 3. Hammett correlation between $\log(K_{aY}/K_{aH})$ and σ_p° at 298 K in $CDCl_3$ for two [2]pseudorotaxanes series **1**·**3a-e** (□, $r^2 = 0.94$) and **1**·**5a-e** (●, $r^2 = 0.82$).

from extended π-systems. This implies that any observed electronic induction occurs through the pyridyl σ-framework, and in our case, is transmitted though the metal-center by way of the nitrogen lone-pair to the chloride co-ligands. The calculated ρ value ($\rho = -0.554$) from Figure 2 indicates a predictable decrease of charge density at the supramolecular reaction center (i.e., chloride ligands) as the donating ability of the pyridine co-ligands decrease. What can be concluded from these results is that a remote substituent can effectively alter the hydrogen-bond acceptor character of the chloride co-ligands, directly influencing the efficacy of chloride ligand recognition by the isophthalamide subunits of **1**.

Assessment of the $K_{1:1}$ values for dibromopalladium(II) complexes (**3a**-**e**) and dichloroplatinum(II) complexes (**5a**-**e**) with **1** reveals a similar trend. An increased ratio of radius to charge and poor steric fit of bromide in the isophthalamide clefts of **1** is likely the cause for such a dramatic decrease in the magnitude of association for this small series of palladium(II) dibromide-based [2]pseudorotaxanes. However, we were particularly interested in the extent of complexation between platinum(II) dichloride axles **5a**-**e** and **1**, compared to the original palladium(II) dichloride series (**1**·**2a**, **1**·**2b**, and **1**·**2h**), as the kinetic stability of platinum(II) complexes could lead to a wider variety of functional supramolecular species based on the molecular recognition of *trans*-$PtCl_2L_2$ compounds by **1**. The study revealed reduced complexation strengths compared to the palladium(II) dichloride series, but overall they remain relatively high, with a value of 4700 ($\pm$49) M^{-1} for **1**·**5e** compared to that of **1**·**2h** (5500 ($\pm$45) M^{-1}). This decrease in affinity can be attributed to platinum's high(er) field strength in comparison to palladium which leaves the chloride ligands with less "anionic" character, effectively diminishing their ability to act as hydrogen bond acceptors. Nevertheless, these K_a values show promise with regard to the development of platinum(II)-based functional materials incorporating elements of this recognition motif.

For purposes of qualitative comparison (solubility problems limited the number of axles examined), $\log(K_{aY}/K_{aH})$ of **1**·**3a-e** and **1**·**5a-e** are plotted against σ_p° (Figure 3), yielding similar linear free energy relationships for both series. The weak-field nature of the bromide ligand, compared to chloride, gives rise to a much steeper slope for the series **1**·**3a-e** ($\rho = -1.63$). This indicates that the observed inductive effects caused by *para*-substitution of the pyridine ligands on the bromide co-ligands are larger than that of its chloride counterpart, even though the association constants themselves are significantly weaker for **1**·**3a-e**. Conversely, the slope of **1**·**5a-e** ($\rho = -0.51$) shows little deviation compared to **1**·**2a-i** (within experimental error), from which we can conclude that, although there is a small overall reduction in complexation strength (mentioned above) for this series of host−guest complexes, the overall effect of pyridine *para*-substitution on the $PtCl_2$ subunit does not differ significantly from the **1**·**2a-i** series.

X-ray Crystallography. In addition to the crystallographic information previously obtained for **1**·**2a**,[12] we can now report the solid-state structures for host−guest complexes **1**·**2h**, **1**·**2i**, and **1**·**5e**. Poor solubility of several of the axle components lead to their selective crystallization from solution with the exception of these three complexes, for which single co-crystals of X-ray quality were obtained. Single crystals were grown from a concentrated chloroform solution containing equimolar amounts of **1** and the respective axle by slow vapor diffusion of diisopropyl ether, and then subjected to single crystal X-ray diffraction analyses. The resulting structural solutions each revealed the desired interpenetrated geometry. **1**·**2h** and **1**·**5e** both crystallized in space group $P2(1)/n$, while **1**·**2i** crystallized in space group $P\bar{1}$ containing two very similar [2]pseudorotaxane superstructures (distances and angles differ slightly) per unit cell.

[2]Pseudorotaxanes 1·2h and 1·5e. Upon examination of their solid-state structures, we were unsurprised to find that host−guest complexes **1**·**2h** and **1**·**5e** crystallized in an isostructural manner (Figure 4). Consequently, these two structures will be discussed together for purposes of brevity. Selected distances and angles are accompanied with Pd or Pt subscripts. The space group ($P2(1)/n$) for structures **1**·**2h** and **1**·**5e** infers that there is a center of symmetry that happens to be located at the metal center. The halide ligands

(30) Mellar, J. W. *A Comprehensive Treatise on Inorganic and Theoretical Chemistry*; Longmans: London, 1936; Vol. 15, p 660.

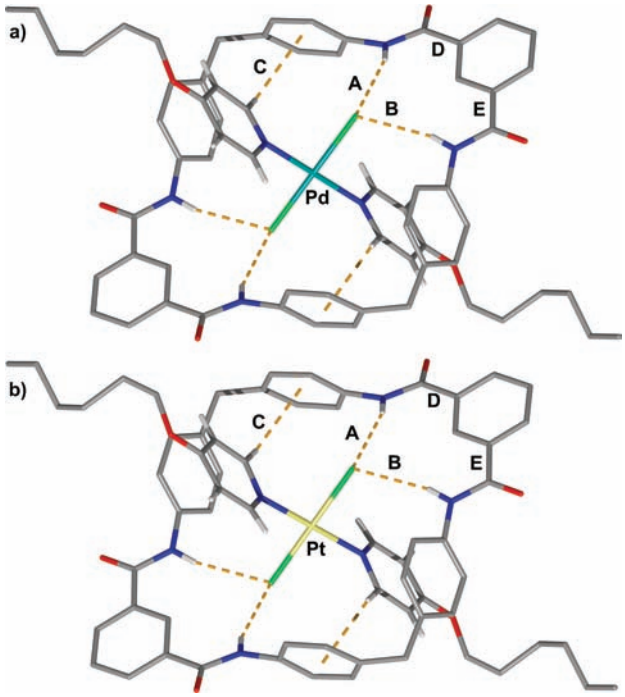

Figure 4. Stick representation of interpenetrated [2]pseudorotaxanes **1·2h** (a) and **1·5e** (b) in the solid state. All C−H hydrogen atoms (exception: pyridyl CH's), methyl, cyclohexyl, and *t*-butyl groups have been removed for clarity. N−H···Cl hydrogen bonds and C−H···π interactions are indicated by orange dashed lines. Color code: C, gray; H, white; N, blue; O, red; Cl, green; Pd, teal; Pt, pale yellow.

of **2h** and **5e** are each engaged in two hydrogen bonds (**A** and **B**) with the amide NH's of **1** (N(40)···Cl (**A**) = 3.22_{Pd} and 3.23_{Pt} Å, N(25)···Cl (**B**) = 3.46_{Pd} and 3.47_{Pt} Å; N(40)−H(40A)···Cl (**A**) = 151_{Pd} and 151_{Pt}°, N(25)−H(25A)···Cl (**B**) = 163_{Pd} and 164_{Pt}°), and both 4-substituted pyridine co-ligands participate in C−H···π interactions (**C**) with the diphenylcyclohexyl sidewalls of **1** (C(6)−H(6A)···π (**C**) = 3.03_{Pd} and 2.98_{Pt} Å). As observed in **1·2a**,[12] both Cl−M−Cl axes are canted in the center of their respective macrocyclic cavities by approximately 25° with respect to the macrocyclic least-squares plane,[19] while diverging from the planes that bisect the aryl-isophthalamide rings[20] by approximately 8° causing the amide groups to deviate from coplanarity (**D** and **E**) in the direction of their respective chloride ligands (torsional angles for C(29)−C(30)−C(38)−N(40) (**D**) = 22_{Pd} and 23_{Pt}°, C(29)−C(28)−C(26)−N(25) (**E**) = 6_{Pd} and 6_{Pt}°). In addition, the *n*-hexyl chains of the axle components adopt an approximate helical conformation (O(71)−C(77)).

[2]Pseudorotaxane 1·2i. The unit cell of **1·2i**, as mentioned above, contains two structurally similar interpenetrated [2]pseudorotaxanes whose contact distances and angles differ slightly. We have only included a graphic (Figure 5) of the superstructure associated with Pd(2) of the unit cell because of this similarity and will again combine descriptions of their individual characteristics to simplify the discussion. The

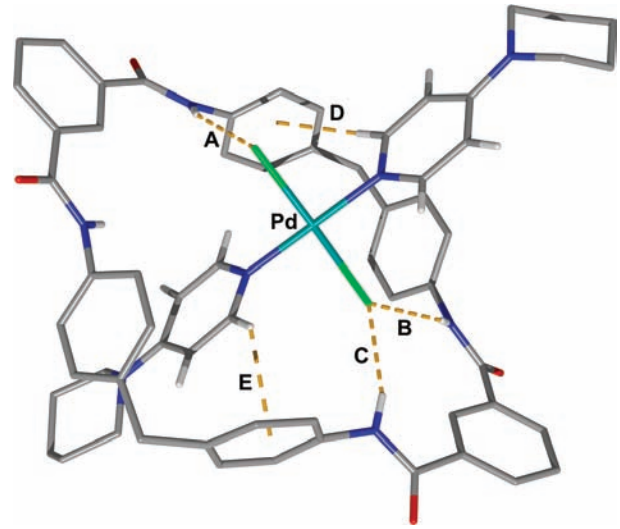

Figure 5. Stick representation of interpenetrated [2]pseudorotaxanes **1·2i** in the solid state. All C−H hydrogen atoms (exception: pyridyl CH's), methyl, cyclohexyl, and *t*-butyl groups have been removed for clarity. N−H···Cl hydrogen bonds and C−H···π interactions are indicated by orange dashed lines. Color code: C, gray; H, white; N, blue; O, red; Cl, green; Pd, teal.

structure of **1·2i** is particularly interesting in that, despite its high association constant in solution (6800 M^{-1}), only three of the four possible hydrogen bonding interactions are present in the solid state ((**A**): N(25A)···Cl(12) = 3.28 Å, N(78B)···Cl(22) = 3.21 Å; (**B**) N(78A)···Cl(11) = 3.29 Å, N(25B)···Cl(21) = 3.24 Å; (**C**) N(63A)···Cl(11) = 3.32 Å, N(40B)···Cl(21) = 3.35 Å; (**A**) N(25A)−H(25A)···Cl(12) = 149°, N(78B)−H(78B)···Cl(22) = 154°; (**B**) N(78A)−H(78A)···Cl(11) = 155°, N(25B)−H(25B)···Cl(21) = 149°; (**C**) N(63A)−H(63A)···Cl(11) = 153°, N(40B)−H(40B)···Cl(21) = 161°). We speculate that this is the result of crystal packing which also forces the disposition of both Pd(1) and Pd(2) from their respective macrocyclic least-squares plane by 1.78 Å and 1.42 Å, causing the three macrocyclic amides engaged in hydrogen bonding with the chloride ligands to deviate from coplanarity by 27−36° in the same direction. C−H···π interactions are also present in these structures; however, this translational displacement of the palladium(II) centers results in one very close contact ((**D**) C(122)−H(12A)···π = 2.85 Å, C(206)−H(20D)···π = 2.39 Å) and one lengthened contact ((**E**) C(102)−H(10A)···π = 3.06 Å, C(222)−H(22A)···π = 3.10 Å). The single amide groups of each [2]pseudorotaxane that do not participate in hydrogen bonds with the chloride ligands display weak hydrogen bond contacts between their carbonyl oxygen atoms and included chloroform molecules (C(700)···O(39A) = 3.22 Å, C(700)−H(70A)···O(39A) = 145°; C(500)···O(65B) = 3.14 Å, C(500)−H(50E)···O(65B) = 156°).

Conclusion

In summary, we have demonstrated that in both solution and the solid state, the present hydrogen bond template strategy is very effective in the formation of interpenetrated host−guest complexes. The hydrogen bond accepting ability of chloride co-ligands on a palladium(II) center can be controlled by the electron donating/withdrawing nature of

(31) (a) Tessier, C.; Rochon, F. D. *Inorg. Chim. Acta* **1999**, *295*, 25. (b) Kauffman, G. B. *Inorg. Synth.* **1970**, *7*, 249.
(32) (a) Anderson, G. K.; Lin, M.; Sen, A.; Gretz, E. *Inorg. Synth.* **1990**, *28*, 60. (b) Kharashr, M. A.; Seyler, C.; Mayor, F. R. *J. Am. Chem. Soc.* **1935**, *60*, 882.

its *para*-substituted pyridine co-ligands, and there is a linear free energy relationship associated with this property. This trend is also apparent in [2]pseudorotaxane formation with analogous dibromopalladium(II) (with reduced K_a) and dichloroplatinum(II) complexes. The effect of pyridine *para*-substitution on the palladium(II) dibromide **1·3a-e** series is greatly enhanced compared to both the palladium(II) and platinum(II) dichloride series that we attribute to the weaker nature of the Pd−Br bond. The solid-state structures of three [2]pseudorotaxanes were presented, further confirming the nature of the originally proposed interpenetrated geometry but containing pyridine ligands with *para*-substituents different from hydrogen. The high kinetic stability of $PtCl_2$-based metal complexes and the reasonably strong complexation affinities for [2]pseudorotaxane formation within the series examined here (**1·5a-e**) indicates that we will likely have access to more useful and robust mechanically bonded analogues given appropriately designed ligands and synthetic techniques.

Acknowledgment. We are grateful for the financial support provided by the Natural Sciences and Engineering Research Council of Canada and the University of Western Ontario.

Supporting Information Available: Crystallographic data in CIF format. This material is available free of charge via the Internet at http://pubs.acs.org.

IC801725U